ACCOUNTS of chemical research

pubs.acs.org/accounts Article

Lanthanide-Activated Nanoparticles: A Toolbox for Bioimaging, Therapeutics, and Neuromodulation

Zhigao Yi, Zichao Luo, Xian Qin, Qiushui Chen, and Xiaogang Liu*

Cite This: *Acc. Chem. Res.* 2020, 53, 2692–2704 Read Online

CONSPECTUS: Owing to their unique features, the past decade has witnessed rapid developments of lanthanide-activated nanoparticles for biological applications. These include highly tunable upconverting and downshifting photoluminescence when illuminated in deep tissue, excellent photostability against blinking and bleaching effects, biocompatibility through versatile surface modification, and ease of achieving multifunctionality, as well as satisfactory signal output. These attributes make lanthanide-doped nanoparticles an ideal toolbox for advanced bioimaging and next-generation therapeutics.

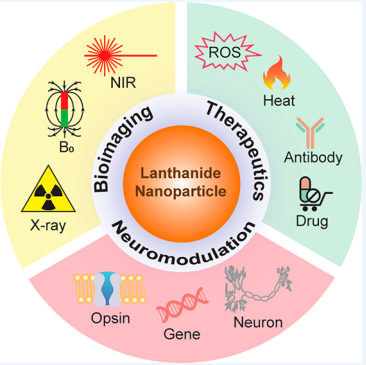

The interest in lanthanide-doped nanoparticles for biomedical research arises from their unique optical properties in response to deep-tissue-penetrable light sources. Upon near-infrared irradiation, these nanoparticles with properly doped emitters display photon upconversion with large anti-Stokes shifts and broad-spectrum tunability from the ultraviolet to the visible. It is also possible to achieve orthogonal photoluminescence with variations in wavelength and lifetime. Coupled with surface ligands, dyes, biomolecules, or other types of functional nanomaterials, lanthanide-doped nanoparticles offer new opportunities for applications in bioimaging, advanced oncotherapy, and neuromodulation. Given the possibility of locating downshifting luminescence at "biological transmission windows", exquisite design of lanthanide-doped nanoparticles also enables deep-tissue imaging with high spatial resolution. In addition, these nanoparticles can respond to high-energy photons, such as X-rays, to trigger nonradioactive and radiative pathways, making it possible to develop high-sensitivity X-ray detectors. Precise control of paramagnetic lanthanide ions in nanocrystal lattices also provides advanced materials for high-performance magnetic resonance imaging in medical diagnostics and biomedical research. Full consideration of fundamental attributes of lanthanide-doped nanoparticles will facilitate the design of multifunctional and sensitive probes and improve diagnostic and therapeutic outcomes.

In this Account, we categorize various lanthanide-activation strategies into three modes: near-infrared excitation, X-ray irradiation, and magnetic field stimulation. We introduce energy manipulations in upconverting, downshifting, and persistence luminescence in spectral and time domains and discuss how they can be applied in biological practices. We assess general design principles for lanthanide-activated nanosystems with multiple modalities of bioimaging, oncotherapy, and neuromodulation. We also review the current state-of-the-art in the field of lanthanide-based theranostic nanoplatforms, with particular emphasis on energy conversion and nano-/biointerfacing as well as emerging bioapplications. In this context, we also highlight recent advances in controlling optical properties of nanoplatforms for single- or multimodal bioimaging, stimulus-responsive phototherapy, and optogenetics. Finally, we discuss future opportunities and challenges of this exciting research field.

KEY REFERENCES

Yi, Z.; Luo, Z.; Barth, N. D.; Meng, X.; Liu, H.; Bu, W.; All, A.; Vendrell, M.; Liu, X. *In Vivo* Tumor Visualization through MRI Off-On Switching of $NaGdF_4$-$CaCO_3$ Nanoconjugates. *Adv. Mater.* **2019**, *31*, 1901851.[1] Self-assembled nanoarchitectures comprising ultrasmall gadolinium nanoparticles and calcium carbonates served as smart contrast agents for high-performance cancer diagnostic imaging in response to the mildly acidic microenvironment in tumor sites.

Mao, D.; Hu, F.; Yi, Z.; Kenry; Xu, S.; Yan, S.; Luo, Z.; Wu, W.; Wang, Z.; Kong, D.; Liu, X.; Liu, B. AIEgen-Coupled Upconversion Nanoparticles Eradicate Solid Tumors through Dual-Mode ROS Activation. *Sci. Adv.* **2020**, *6* (6), eabb2712.[2] A hybrid upconversion system combined with aggressive induced emissive molecules was designed for precision nanomedicine with the modulation of excitation power density to optimize the outcomes of cancer immunotherapy.

Received: August 10, 2020
Published: October 26, 2020

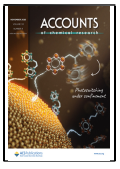

https://dx.doi.org/10.1021/acs.accounts.0c00513
Acc. Chem. Res. 2020, 53, 2692–2704

Chen, S.; Weitemier, A. Z.; Zeng, X.; He, L.; Wang, X.; Tao, Y.; Huang, A. J.; Hashimotodani, Y.; Kano, M.; Iwasaki, H.; Parajuli, L. K.; Okabe, S.; Teh, D. B. L.; All, A. H.; Tsutsui-Kimura, I.; Tanaka, K. F.; Liu, X.; McHugh, T. J. Near-Infrared Deep Brain Stimulation via Upconversion Nanoparticle-Mediated Optogenetics. *Science* **2018**, *359*, 679−684.[3] This lanthanide-activated upconversion investigation realized remote delivery and *in situ* transduction of near-infrared light to stimulatory visible light in the deep brain for wireless and noninvasive neuromodulation in intact animals.

Zeng, X.; Chen, S.; Weitemier, A.; Han, S.; Blasiak, A.; Prasad, A.; Zheng, K.; Yi, Z.; Luo, B.; Yang, I. H.; Thakor, N.; Chai, C.; Lim, K. L.; McHugh, T. J.; All, A. H.; Liu, X. Visualization of Intra-Neuronal Motor Protein Transport through Upconversion Microscopy. *Angew. Chem., Int. Ed.* **2019**, *58*, 9262−9268.[4] Silica-coated upconversion nanoprobes contributed to real-time tracking of cargo trafficking in sensory neurons, implicating the feasibility for the diagnosis of neuro-degenerative disorder.

1. INTRODUCTION

While the phenomenon of lanthanide luminescence was discovered by Bunsen over a century ago, luminescence theories were not systematically established until the 1960s.[5] With the advent of nanotechnology in the past two decades, researchers now can synthesize and characterize lanthanide-doped nanocrystals with desired structures and functions. The fabrication and characterization technologies have permitted exploration of these optical nanomaterials in both fundamental research and technology development. In particular, lanthanide-activated nanoparticles have attracted considerable interest for applications in three-dimensional displays, lasing, super-resolution microscopy, anticounterfeiting, and biomedicine, especially in molecular bioimaging, oncotherapy, and optogenetic neuromodulation.[1−4,6]

The potential of lanthanide-doped nanoparticles for biomedical applications is largely attributable to photon upconversion processes by which upconverted ultraviolet-to-visible light (400−700 nm) can be generated through radiative transitions upon near-infrared (NIR, e.g., 808 and 980 nm) laser irradiation. This approach has two attractive features. One is the ease of combining various dyes, molecules, and functional moieties with upconversion nanoparticles, because full-spectrum adjustability of upconversion emission satisfies rigorous requirements of biological stimuli-response in photo-mediated biosensing and imaging as well as in therapeutics. The other is the ease with which photoactivation can be achieved under remote control, enabling noninvasive, less phototoxic imaging or sensing. The most widely used host materials are sodium rare-earth fluoride (formulated as $NaREF_4$) with relatively low phonon energy. However, lanthanide ions feature narrow absorption cross sections and inefficient nonlinear multiphoton processes. To address these inherent limitations, many strategies have been developed, including host-lattice modulation, molecular sensitization, core−shell engineering, energy transfer/migration manipulation, plasmon resonance enhancement, photonic crystal, and microlens amplification (Figure 1). Additionally, lanthanide-doped nanoparticles also feature downshifting luminescence and programmable radiative decay profiles, expanding their multidimensional emissions in terms of wavelength and lifetime.[7,8] From the perspective of multiplexing activation, lanthanide ions also respond to X-rays and magnetic fields because of their relatively high atomic numbers and distinctive spin−orbital configurations. All these features promise lanthanide-activated nanoplatforms as ideal probes for many applications in precision nanomedicine. Here, we provide an overview of their applications in bioimaging, stimuli-response, oncotherapy, and wireless neuromodulation.

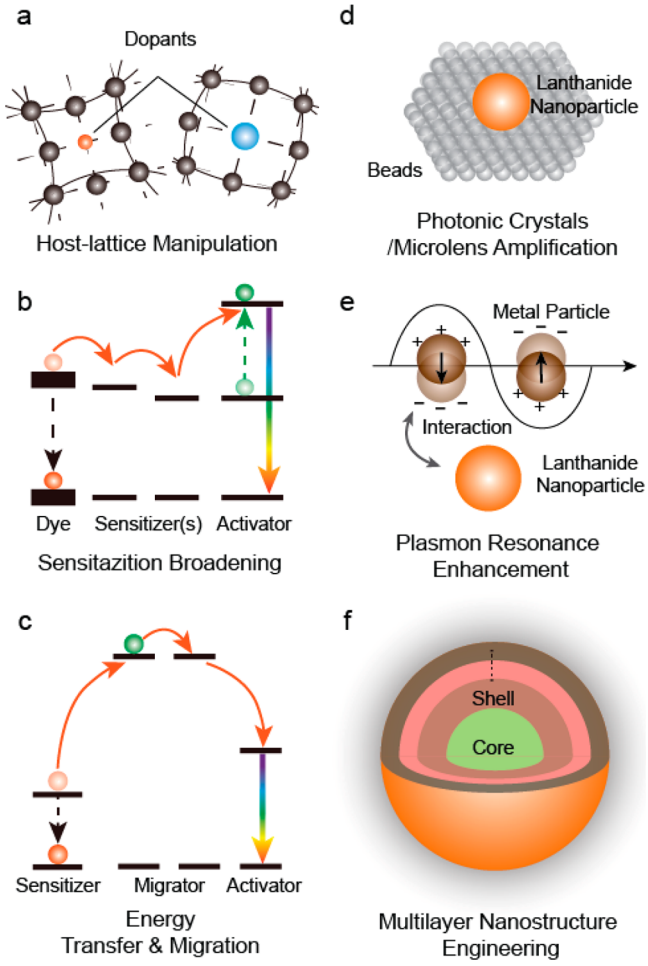

Figure 1. Illustrative graphs showing general strategies to photoluminescence enhancement in lanthanide-activated nanoparticles. (a) Dopant ions in host lattices generate variations in the coordination environment and crystal field splitting, lowering the symmetry of adjacent lanthanides. (b) Molecular dyes with band gaps that well match the energy levels of lanthanides promote the sensitization process. (c) Photon energy can be transferred and migrated over a long distance in nanoparticles with migrators (e.g., Gd^{3+} and Yb^{3+}). (d) Photonic crystals of microbeads can increase the density of incident photons and enhance lanthanide emission. (e) Surface plasmon resonance from metal nanoparticles generates intense electromagnetic fields and boosts the efficiency of energy transfer between lanthanide ions. (f) Core−shell nanostructures provide spatial confinement of lanthanide ions in a nanoparticle.

2. BIOIMAGING

2.1. Near-Infrared Activated Bioimaging

Lanthanide-activated nanoparticles doped with a combination of sensitizers (e.g., Yb^{3+}, Nd^{3+}) and activators (e.g., Er^{3+}, Ho^{3+}, Tm^{3+}) are excitable using 980 or 808 nm lasers to emit light in

https://dx.doi.org/10.1021/acs.accounts.0c00513
Acc. Chem. Res. 2020, 53, 2692−2704

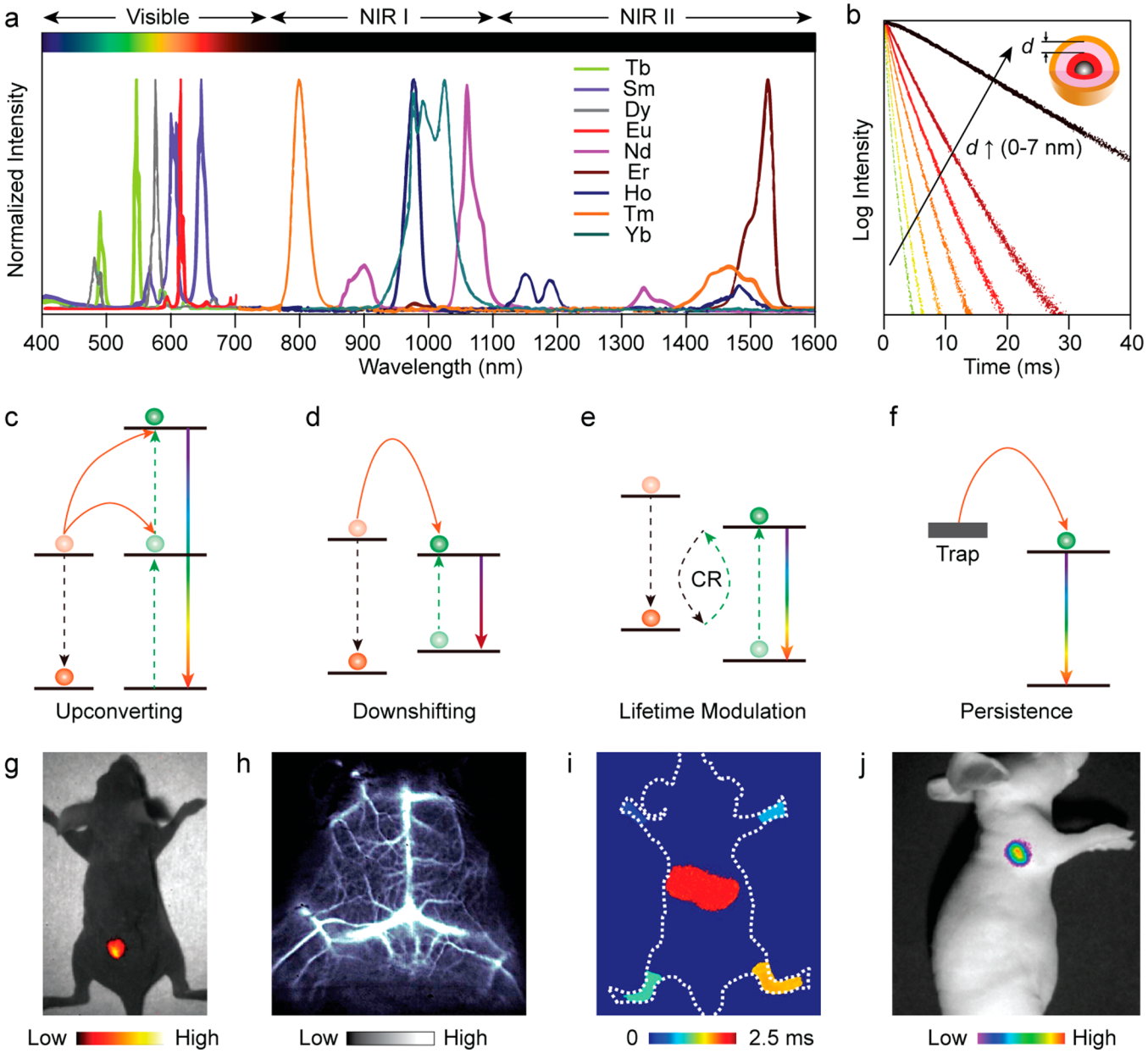

Figure 2. Near-infrared activated lanthanide luminescence in bioimaging. (a) Emission peaks of various lanthanide ions under near-infrared irradiation. (b) Luminescence decay profiles of Er^{3+}-based nanoparticles with thickness variation of a Yb^{3+}-enriched interlayer, recorded at 1532 nm. Principal diagrams showing (c) upconverting emission, (d) downshifting emission, (e) lifetime modulation, and (f) persistent luminescence in lanthanide-doped nanoparticles. (g) Photoluminescence imaging using Nd^{3+}-sensitized nanoparticles under 808 nm irradiation. (h) Cerebral vascular imaging with detection of enhanced Er^{3+} emission at 1532 nm through Ce^{3+} mediation. (i) Time-gated imaging of a nude mouse with injection of nanoparticles having different emission lifetimes in four footpads and through the tail vein. (j) Persistent luminescence detected in lymph nodes of a nude mouse after injection of nanoparticles preactivated at 980 nm. Adapted with permission from ref 9, Copyright 2010 Elsevier; ref 7, Copyright 2018 Macmillan Publishers Limited; ref 11, Copyright 2013 American Chemical Society; ref 17, Copyright 2017 Macmillan Publishers Limited; ref 8, Copyright 2019 Macmillan Publishers Limited; and ref 20, Copyright 2017 American Chemical Society, respectively.

the spectral range from the ultraviolet to the NIR with tunable lifetimes (Figure 2a,b).[7,9] In 2013, several groups demonstrated efficient upconversion emissions using Nd^{3+} as a sensitizer under 808 nm excitation.[10,11] This Nd^{3+}-sensitization strategy largely suppressed the overheating induced by 980 nm excitation with Yb^{3+} sensitization (Figure 2c,g).[11] To further broaden lanthanide activation, an Er^{3+}-sensitized upconversion nanosystem through Tm^{3+} transient energy trapping was developed, the feasibility of which was demonstrated in *in vivo* luminescent imaging under multiwavelength excitation at 808, 980, and 1532 nm.[12] The capacity for multiplex excitation and emission of different lanthanide ions makes them useful to achieve orthogonal photoluminescence in one nanoparticle with a rational core−shell structure.[13] Such an orthogonal-upconversion system provides the concept of an all-in-one nanoplatform with multiple excitation inputs and outputs, which is valuable for programmable and optical manipulation of biological processes in biosensing, imaging, phototherapy, and optogenetics.

On upconversion emission enhancement, we and many others verified that multilayered nanostructures represent the most basic and widespread strategy to precisely manipulate

https://dx.doi.org/10.1021/acs.accounts.0c00513
Acc. Chem. Res. 2020, 53, 2692−2704

energy transfer and migration pathways through the confinement of lanthanide ions in specific nanospaces.[6] In addition, we also reported the utilization of dielectric microbeads to enhance photon upconversion processes in lanthanide-doped nanocrystals.[14] By modulating the wavefront of both excitation and emission fields through dielectric superlens effects, luminescence amplification of more than 5 orders of magnitude can be achieved at a pumping power density of 1.5 W/cm^2. By utilizing cavity-supported plasmon resonance mode, we amplified upconversion luminescence by 4−5 orders of magnitude with a fast-spontaneous emission rate of sub-2 μs lifetime.[15] Despite the remarkable enhancement by these two strategies, there is still a challenge to adapt them for *in vivo* applications.

Despite considerable progress, conventional *in vivo* upconversion luminescence imaging suffers from inevitable limitations in sensitivity and resolution because of the large absorption and scattering effects of biotissues on emitted visible light. To address these concerns, new luminescence imaging modes are exploited to (i) downshift detection wavelengths to the second near-infrared window (Figure 2d) and (ii) modulate emission lifetime to achieve time-domain imaging (Figure 2e). In 2015, our report on non-steady-state upconversion tuning through Ce^{3+}-mediation indicated the feasibility of manipulating the downshifting of emissions.[16] In 2017, Zhong et al. reported Er^{3+}/Ce^{3+} codoped β-phase $NaYbF_4$ nanocrystals for luminescence imaging beyond 1500 nm.[17] In their study, Ce^{3+} doping simultaneously suppressed photon upconversion and boosted competitive downshifting decays, resulting in fast *in vivo* imaging of blood vasculature in the brain (Figure 2h). Another investigation on Er^{3+}/Ce^{3+} codoped nanosystems further verified the ability to optically visualize tiny tumors of ∼4 mm and their vessels with a high spatial resolution of 41 μm.[18] In 2019, Zhong et al. found that α-phase $NaYbF_4$ is a better host material than its β-phase counterpart for downshifting luminescence, in which an 11-fold enhancement in the NIR-II region was achieved by using the α-phase $NaYbF_4$ host with Zn^{2+} dopants.[19] This optimized nanoplatform offers a signal-to-noise ratio of 40. In contrast to diverse strategies for upconversion emission enhancement, in theory there is ample room to optimize downshifting luminescence in lanthanide nanocrystals because of the higher quantum efficiency of downshifting relative to multiphoton upconversion. However, one concern is the sharp decrease in NIR emission of nanoparticles after hydrophilic modifications.[17] Another concern is that most extant luminescent dyes, biomolecules, and other functional biomotifs match well with upconverting emissions in the visible region rather than downshifting emissions in the near-infrared I and II regions, which hinders wide bioapplications of these downshifting nanoprobes.

In 2018, in combination with downshifting luminescence, Fan et al. developed a lifetime-tunable imaging nanoplatform by manipulating Yb^{3+}-mediated energy migration in a multilayered core−shell nanostructure.[7] This time-domain multiplexing outperformed the corresponding intensity-domain imaging mode with a single emission band that varied by 3 orders of magnitude, revealing its potential for quantitative *in vivo* imaging and disease diagnosis. In 2019, Gu et al. exploited a pristine Yb^{3+}-hosted nanoparticle as a light transducer, in which long-decaying luminescence of Yb^{3+} at 980 nm with an efficiency approaching 100% was achieved under the same wavelength excitation (Figure 2i).[8] Benefiting from this time-domain scheme, this nanoprobe was successfully applied to high-contrast (>9) *in vivo* imaging at a relatively low dosage of 13 μg/g and an excitation power of 1.1 mW/cm^2. Integration of near-infrared emission and time-domain imaging efficiently improves the sensitivity of bioimaging, especially in deep-tissue.

Additionally, persistent luminescence could be an attractive approach to achieve high-performance optical imaging, since such nanoprobes can store energy through pre-excitation and emit light spontaneously without irradiation during imaging processes (Figure 2f,j).[20] Therefore, this technique could effectively circumvent irradiation-induced background noise, heating effects, and resulting biological damage. However, there are no robust methods to synthesize persistent nanoprobes with both homogeneous size and high-performance persistent luminescence. The general process of calcination at high temperatures leads to reduced amounts of ligands remaining on particle surfaces and the resultant difficulty of postmodification.

2.2. X-ray Imaging

Lanthanide ions present high K-edge values and X-ray coefficients due to their high atomic numbers, which enable efficient absorption of X-rays for planar and computed tomography imaging (Figure 3a). For example, Yb^{3+}-based

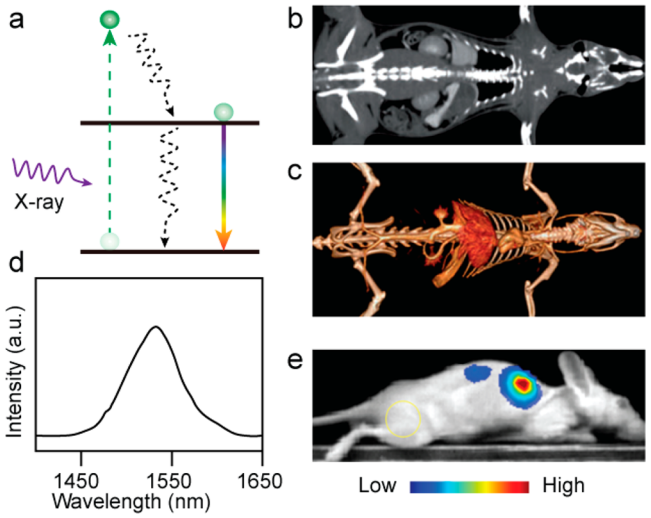

Figure 3. Lanthanide-activated nanoparticles for X-ray-enabled bioimaging. (a) Nonradiative and radiative decays of lanthanide-doped nanoparticles under X-ray irradiation. (b) Planar and (c) computed tomography X-ray imaging using Yb^{3+}-based nanoparticles. (d) X-ray-excited emission spectrum and (e) luminescence imaging in the near-infrared IIb region of Er^{3+}-doped nanoparticles. Adapted with permission from ref 21, Copyright 2012 WILEY-VCH Verlag GmbH & Co. KGaA; and ref 22, Copyright 2014 American Chemical Society, respectively.

nanoprobes presented outstanding attenuation characteristics and offered a higher contrast performance on *in vivo* angiography and lymph node mapping at 120 kVp, compared with clinically iodinated agents (Figure 3b,c).[21] In addition to energy annihilation, lanthanide-doped nanoparticles also exhibit X-ray scintillation characteristics that convert absorbed X-rays to light emission. In 2015, Naczynski et al. found that conventional Yb^{3+}/Er^{3+} codoped $NaYF_4$ nanocrystals can emit light at ∼1530 nm under X-ray irradiation (Figure 3d,e).[22] This energy conversion from X-ray to near-infrared-II light was

https://dx.doi.org/10.1021/acs.accounts.0c00513
Acc. Chem. Res. 2020, 53, 2692−2704

used to monitor the biodistribution of nanoprobes *in vivo* and to map lymphatic drainage. Apart from their X-ray response, lanthanide-doped nanocrystals can also be activated by energetic charged particles. In 2015, our group demonstrated α-beam excited upconversion for cellular structure mapping with a high spatial resolution of sub-30 nm.[23] Currently, X-ray-related imaging techniques and proton therapy are popular in clinical practice. The development of lanthanide-based contrast agents helps address safety concerns about the overdosage of high-energy irradiation and induced adverse effects such as radical accumulation in the body.

2.3. Magnetic Resonance Imaging

Lanthanide ions with unpaired 4f electrons are paramagnetic, thereby responding to external magnetic fields. In this regard, lanthanide-doped nanoparticles can serve as contrast agents to shorten relaxation times of surrounding protons and subsequently enhance contrast in magnetic resonance imaging (Figure 4a). In general, signals are assessed based on either

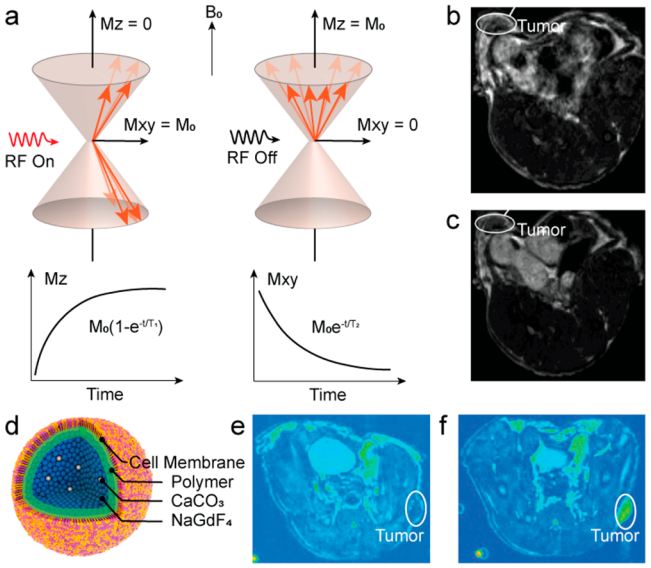

Figure 4. Lanthanide-activated nanoparticles for magnetic resonance imaging. (a) Change of electron spin of protons with and without radio frequency (RF) and resultant variations of magnetization in longitudinal and transversal directions. (b, c) T_2-weighted tumor imaging before and after administration of $NaDyF_4$ nanoparticles. (d) Design of pH-responsive contrast agents for T_1-weighted imaging, and performance on *in vivo* tumor visualization (e) before and (f) after nanoparticle injection. In this design, the embedded $CaCO_3$ nanoparticles quickly respond to the mildly acidic microenvironment at tumor sites and then generate gases to disrupt the nanostructure. The local release of abundant $NaGdF_4$ nanoparticles triggers T_1 signals through efficient interactions between Gd^{3+} ions and water protons. Adapted with permission from ref 25, Copyright 2016 American Chemical Society; and ref 1, Copyright 2019 WILEY-VCH Verlag GmbH & Co. KGaA, respectively.

positive or negative effects, corresponding to the readout of brighter images in the T_1-weighted imaging mode or of darker images in the T_2-weighted imaging mode. Of lanthanide ions with open-shell configurations, Gd^{3+} is an ideal T_1 agent while others (Dy^{3+}, Ho^{3+}, Er^{3+}, Tm^{3+}, and Yb^{3+}) are suitable as T_2 agents, depending on their ability to vary longitudinal and transverse relaxation times of surrounding protons.

In 2014, Xing et al. reported 2 nm $NaGdF_4$ nanodots coated with PEG and DTPA for efficient angiography and atherosclerotic plaque imaging in T_1-weighted mode.[24] In this study, ultrasmall size and PEG coating endowed a rapid excretion of nanoagents from the body, and DTPA chelating prevented leakage of free Gd^{3+} ions. In 2016, a report by Zhang et al. indicated that pristine $NaDyF_4$ and $NaHoF_4$ nanoparticles are promising candidates as T_2-agents, especially under a high magnetic field of 9.4 T (Figure 4b,c).[25] In addition, binary contrast agents for the *in vivo* T_1/T_2 dual-weighted imaging mode can also be achieved by controlling the dopant concentration in nanocrystals.[26] In 2019, our group designed a nanoconjugate through self-assembly of ultrasmall $NaGdF_4$ and $CaCO_3$ nanoparticles to realize on-demand T_1 signal amplification in response to mildly acidic conditions at tumor sites (Figure 4d–f).[1] Encapsulating cancer cell membranes on nanoconjugate surfaces, the probes homologously targeted tumor sites *in vivo* and exhibited a 60-fold imaging signal enhancement over a clinical agent, Magnevist. Although many lanthanide-nanoparticle-based contrast agents exhibited better *in vivo* performance for cancer diagnosis in animal models over molecule-based clinical agents, there is still a long way to clinical translation in terms of biosafety assessment.

It should be mentioned that every bioimaging technique possesses advantages and disadvantages. Specifically, luminescence imaging offers visualization of morphological details of individual cells, organs, and whole organisms with high spatial resolution, while the penetration depth of light is limited within millimeter to centimeter scales. X-ray imaging provides both structural and functional information on targeted regions with ideal spatial resolution. The downside of this technique is the need for high dosages of agents. Magnetic resonance imaging carries out functional implications but suffers from limited spatial resolution. Given these, integrating all functions of a single imaging modality into one type of nanoprobe could be effective to precisely localize lesions through multimodal imaging or multiple purposes in disease diagnosis and treatment.

3. ONCOTHERAPY

3.1. Stimuli Response to the Tumor Microenvironment

The generation and growth of tumors require new blood vessels for oxygen and nutrient supplies. In comparison with regular blood vessels, proliferated vessels inside and surrounding tumors feature abnormal structures, such as poor lymphatic drainage and disorganized, leaky vasculature. These are crucial factors that lead to penetration and retention of nanoparticles and macromolecular drugs at tumor sites, a phenomenon well-known as the enhanced permeability and retention (EPR) effect. The microenvironment of tumor tissues also exhibits acidic pH, hypoxia, and redox reactants, which have been widely utilized to design smart lanthanide-activated nanoprobes for tumor-targeting imaging and therapeutics. Alternative strategies for personalized lanthanide nanomedicine have also been exploited to respond to unique characteristics of intracellular signals of tumor cells, such as excessive levels of adenosine triphosphate (ATP), metal ions, biomarkers, and metabolites.

As for the pH response, proton-sensitive diblocked polymers, supramolecules, and peptides are generally conjugated onto surfaces of lanthanide-doped nanoparticles to realize on-demand drug release or signal amplification.[27] Nontoxic inorganic nanomaterials that are responsive to acidic

https://dx.doi.org/10.1021/acs.accounts.0c00513
Acc. Chem. Res. 2020, 53, 2692–2704

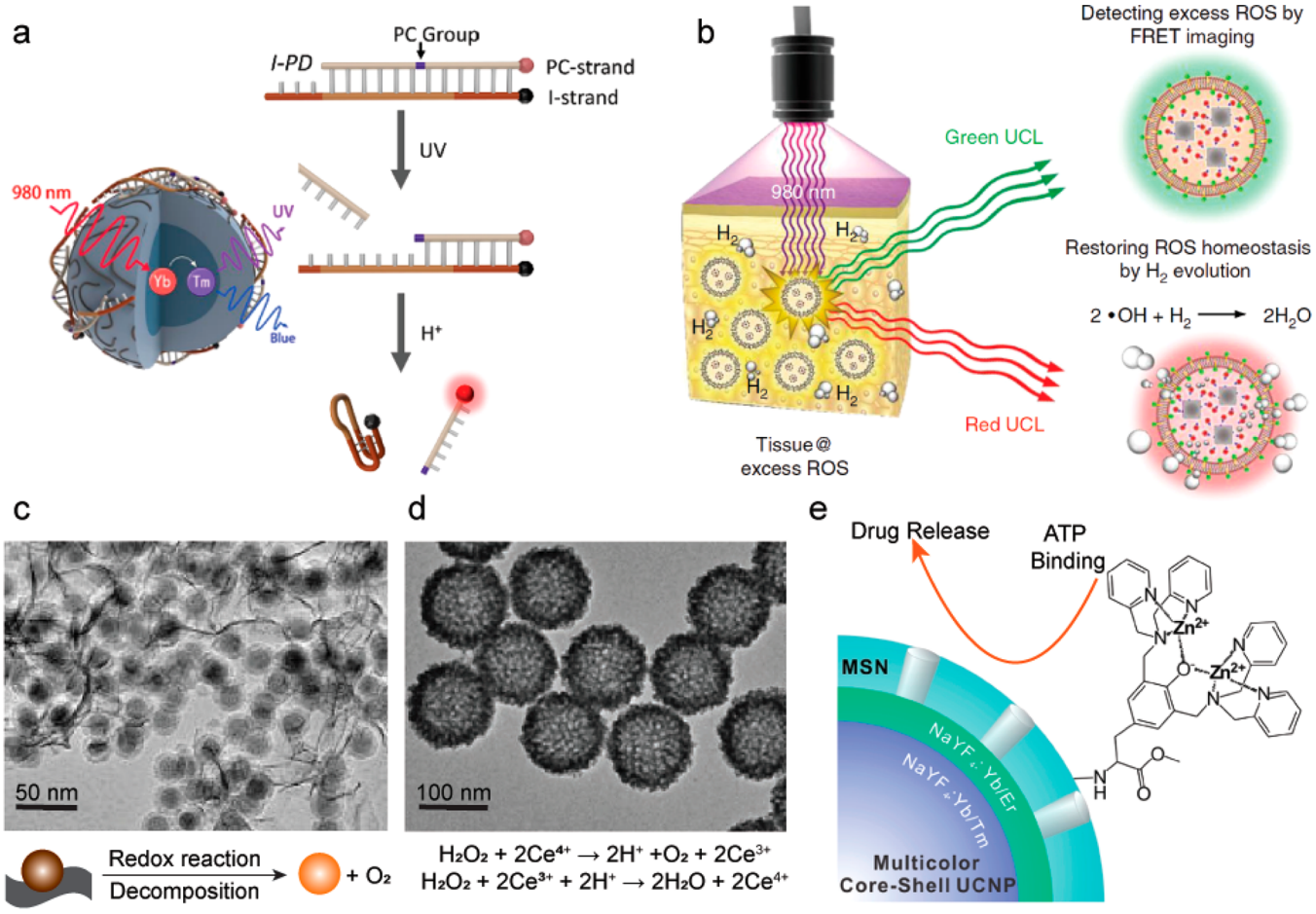

Figure 5. Lanthanide-activated nanoparticles responsive to the tumor microenvironment. (a) Schematic structure of a photoactivatable DNA nanomachine and the working mechanism for programmable pH sensing. (b) Schematic mechanism of a photodriven H_2-evolving liposomal nanoplatform. Green and red upconverted emissions of the nanoplatform can be used for simultaneous detection and reduction of excess ROS species *in situ*. Typical transmission electron microscope images of (c) MnO_2 nanosheet-anchored lanthanide-nanoparticles and (d) mesoporous lanthanide-doped CeO_2 hollow structures, and their corresponding mechanisms to O_2 generation. (e) Schematic zinc dipicolylamine (TDPA-Zn^{2+}) bonding to nanoparticle surfaces. The presence of ATP triggers the release of drugs stocked in mesoporous holes through competitive interactions between ATP and TDPA-Zn^{2+}. Adapted with permission from ref 29, Copyright 2020 American Chemical Society; ref 33, Copyright 2020 Macmillan Publishers Limited; ref 36, Copyright 2015 WILEY-VCH Verlag GmbH & Co. KGaA; ref 37, Copyright 2018 WILEY-VCH Verlag GmbH & Co. KGaA; and ref 40, Copyright 2015 American Chemical Society, respectively.

conditions (e.g., $CaCO_3$ and ZnO) can also functionalize lanthanide-activated nanoparticles to amplify diagnostic signals on demand through self-dissolving nanostructures at tumor sites.[1,28] However, pH-responsive behavior in these designs is not selective for tumor cells. The passive-targeting (EPR) effect or specificity necessitates the addition of active-targeting motifs to nanoparticles for tumor accumulation and signal amplification. A recent study showed that a nanomachine comprising double-stranded DNA and ultraviolet emissive upconversion nanoparticles can selectively monitor pH variation in live cells and animals (Figure 5a).[29] In contrast to the conventional design of pH-responsive nanoparticles, this nanomachine only responded to pH after selective photoactivation of DNA motifs by ultraviolet emissions from upconversion nanoparticles, which enabled pH sensing in a programmable manner.

Tumor hypoxia reduces the susceptibility of cancer cells to antineoplastic drugs, slows responses to free radicals, and restricts anticancer effectiveness of photodynamic therapy due to oxygen consumption during therapy. Several strategies involving lanthanide-activated nanoparticles have been established to address these concerns. One is to deliver extra oxygen to tumor sites in order to offset the fast consumption of oxygen during photodynamic therapeutic processes. A recent study demonstrated a natural oxygen microcarrier comprising hypoxia probes, red blood cells, and upconversion nanoparticles.[30] This microcarrier efficiently evaded uptake by the reticuloendothelial system, improved accumulation at tumors, selectively delivered oxygen in hypoxic regions under photostimulation, and provided sufficient oxygen for photodynamic therapy. On the other hand, hypoxia can be also utilized for targeted tumor imaging and treatment. A recent study innovatively exploited colonization of anaerobic bacteria under reduced oxygen, in which selective delivery of bacterial−nanoparticle hybrids to the hypoxic regions of tumors prolonged diagnosis and therapy.[31] In contrast, anoxic surroundings of tumors may contribute to inhibition of tumor growth and metastasis through bioreductive therapy because bioreductive prodrugs usually become highly cytotoxic after activation under hypoxic conditions. For example, a hybrid nanoplatform comprising upconversion nanoparticles, photosensitizers, and bioreductive prodrugs showed synergistic

https://dx.doi.org/10.1021/acs.accounts.0c00513
Acc. Chem. Res. 2020, 53, 2692−2704

antitumor effects under near-infrared irradiation, compared with photodynamic therapy alone.[32] However, nanoprobes are usually injected into tumors to achieve the best therapeutic performance, which narrows their wide application in clinics.

Normally, pathogenesis involves an imbalance of highly cytotoxic reactive oxygen species (ROS), such as hydroxyl radical ($^{\bullet}OH$), superoxide anion radical ($^{\bullet}O_2^-$), and singlet oxygen ($^1O_2$). Intracellular ROS generated from partial reduction of oxygen acts as secondary messengers in regulating cell signaling, protein functions, and inflammation. As such, redox-responsive lanthanide nanoprobes have been exploited to monitor ROS in real-time through fluorescence resonance energy transfer (FRET) methodology and to regulate ROS through photosensitizing dynamics, to combat diseases, including malignancies, cardiovascular dysfunctions, and neurological disorders. As for ROS sensing, a thioketal-based linker responsive to H_2O_2 was used to assemble gold and upconversion nanoparticles (Figure 5b).[33] In this study, the presence of H_2O_2 led to detachment of gold nanoparticles from nanoparticle surfaces, resulting in the recovery of green emission. In addition, the red emission of upconversion nanoparticles facilitated chlorophyll α-mediated photosynthesis of H_2 gas to scavenge excess local ROS. Recently, our group also developed a colorimetric method to achieve real-time *in vivo* monitoring of the hepatoxicity of synthetic drugs through a cyanine-peroxynitrite ($ONOO^-$) reaction.[34] In this work, chromophore-conjugated upconversion nanoprobes offered $ONOO^-$ detection at the limit of 0.08 M and a fast analyte response less than 1 s. Despite numerous studies on ROS sensing, it is still difficult to recognize and quantitatively detect subtypes of ROS using these nanoparticle-based approaches.

In regard to redox status manipulation, lanthanide-based nanotechnology has been focused on enriching ROS generation and reducing ROS scavenging in targeted cells, as well as on maintaining homeostasis in healthy cells. For instance, metal−organic frameworks and titanium dioxide-functionalized upconversion nanoparticles were developed to enhance ROS generation through both electron and energy transfer processes.[35] MnO_2 nanosheets and CeO_2 nanoparticles have been devoted to supplying oxygen *in situ* to offset tumor-induced hypoxia, which complicates photodynamic therapy (Figure 5c,d).[36,37]

In addition, enhancing ROS accumulation in tumor cells by inhibiting its scavenging is an attractive approach. To this end, a small synthetic molecule ($C_{17}H_{14}BrF_2N_3OS$) was recently utilized to target and bind intracellular copper-trafficking proteins such as Atox1 and CCS, inhibiting copper transfer to specific destinations.[38] Reduced consumption of ROS resulted from downregulation of glutathione (GSH), nicotinamide adenine dinucleotide phosphate (NADPH), and superoxide dismutase (SOD1). Alternatively, spatiotemporal regulation of intracellular ROS using a bifunctional C_{60}-capped upconversion nanoplatform was effective for the treatment of Alzheimer's disease, in which C_{60} served as both an ROS generator and scavenger.[39] In this case, ROS generation by C_{60} under photoactivation promoted photo-oxygenation of neurotoxic amyloid-β peptides and inhibited their aggregation, while consumption of ROS by C_{60} in the dark prevented increased oxidative stress.

ATP, the energy currency for intracellular energy transfer, provides energy to various biological processes in living cells. There is an abnormal upregulation of ATP in cancer tissues because a massive supply of energy is indispensable for cancer growth. Therefore, ATP overproduction in tumor tissues can be applied to stimulus-responsive nanoplatform design. Recently, polypeptide/TDPA-Zn^{2+}-capped mesoporous upconversion nanoparticles loaded with drugs were synthesized for ATP-responsive drug release (Figure 5e).[40] This design made use of the high binding affinity of ATP to the surface-capped TDPA-Zn^{2+} over polypeptides, which led to ATP-triggered drug release through polypeptide substitution. However, one concern about this nanoplatform is its nonselectivity in the presence of ATP. To achieve spatiotemporal responsiveness triggered by ATP, an upconversion-activatable nanodevice coupled with double-stranded DNA was developed.[41] In this design, successful ATP-response requires that the photocleavable group first be unlocked in the complementary DNA strand through upconverted ultraviolet emission, followed by binding of ATP to the exposed aptamer probe.

3.2. Photodynamic Therapy

Photodynamic therapeutics mainly induces apoptosis of cancer cells through ROS generation. Current challenges involve three key components: photosensitizers, excitation light, and oxygen sources. However, most photosensitizers suffer from insufficient generation of ROS, poor solubility, and inadequate biocompatibility. Ultraviolet or visible light typically used for photoreactions has limited ability to penetrate deep tissue. The hypoxic microenvironment in the centers of solid tumors is another limiting factor. To address these concerns, the structural design and surface engineering of lanthanide-activated nanoparticles enable remote and noninvasive delivery of stimulatory light to deep lesions, physiochemical and optical stabilization of photosensitizers, and even extra functionalities to combat tumor microenvironmental characteristics, such as hypoxia. To enlarge the photoconversion efficacy, multilayered, core−shell nanostructures are usually employed to combat concentration and surface quenching effects. To suppress overheating from irradiation sources, photon absorbers, such as dyes or other types of lanthanide ions, are alternatives. Engineering nanoprobes with pre-existing or *in situ* generated superstructure also improves therapeutic performance. A recent example of self-assembling upconversion nanoparticles using pH-responsive polymer ligands revealed on-demand generation of ROS in deep tissue and enhanced therapeutic efficacy, where the photosensitizer was initially self-quenched in the confined superstructure and released after pH-activation.[42] *In situ* aggregation of nanoprobes in tumor cells promoted $^1O_2$ generation as a result of enhanced photosensitization, in which covalent cross-linking between nanoparticles was conducted by exposing cysteine and 2-cyanobenzothiazole via tumor-specific cathepsin enzyme reactions.[43] Photodynamic nanotheranostics have also been used to target tumors by introducing various targeting ligands and antibodies to nanoparticle surfaces. Recent research demonstrated that assembling multiple building blocks into one nanoplatform triggered a cascade reaction during therapeutic dynamics in which gold, upconversion nanoparticles, and metal−organic frameworks generated H_2O_2, O_2, and $^1O_2$, respectively.[44] Although upconversion nanoplatform-based photodynamic therapy shows promise for inhibition of tumor growth, it still suffers from low efficacy in treating large tumors, high risk of irradiation-induced damage to healthy cells, and limited effects on metastatic tumors.

https://dx.doi.org/10.1021/acs.accounts.0c00513
Acc. Chem. Res. 2020, 53, 2692−2704

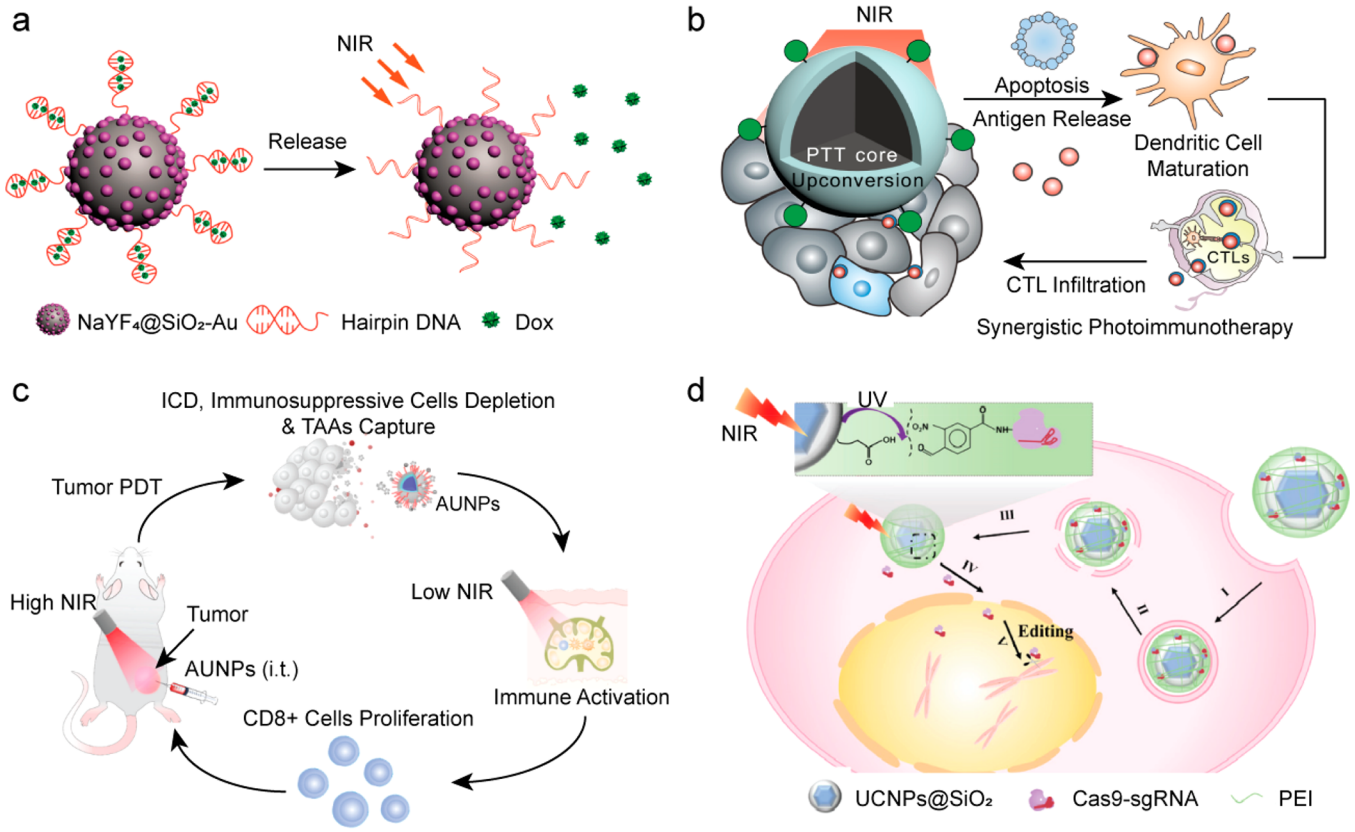

Figure 6. Schemes of lanthanide-activated nanoparticles in phototherapy. (a) Upconversion emission-induced drug release system through gold and hairpin DNA functionalization. (b) Synergistic photodynamic and photothermal therapy for augmentation of antitumor immunity using polydopamine-upconversion nanocomposites. (c) Near-infrared irradiative density-dependent immunotherapy through AIEgen-coupled upconversion nanoparticles (AUNPs). (d) Lanthanide-activated gene editing nanoplatform based on remote control of near-infrared irradiation. Adapted with permission from ref 48, Copyright 2019 WILEY-VCH Verlag GmbH & Co. KGaA; ref 2, Copyright 2020 American Association for the Advancement of Science; ref 45, Copyright 2017 WILEY-VCH Verlag GmbH & Co. KGaA; and ref 53, Copyright 2019 American Association for the Advancement of Science.

3.3. Photothermal Therapy

Photothermal treatment lies in the conversion of absorbed photons to vibrational energy in the form of heat. To this end, one of the key points of nanotheranostic platform design is to enhance the photothermal conversion yield. For example, ideal thermal transductors, such as gold and iron oxide nanoparticles, can be conjugated onto the surfaces of lanthanide-activated nanoparticles to improve photothermal conversion efficacy. Our group recently developed a multifunctional upconversion nanoconjugate comprising hairpin DNA and Au nanoparticles, in which hairpin DNA strands served as stabilizers to improve the biocompatibility of nanoconjugates, and ultrasmall Au nanoparticles efficiently converted visible emissions to heat and triggered *in vivo* drug release (Figure 6a).[45] In photothermal therapy, overheating must be carefully considered because it may damage normal cells and tissues around lesions. It is therefore essential to accurately monitor heating at specific sites, such as tumors. By taking advantage of temperature-sensitive optics of upconversion nanoparticles, a nanocomposite with temperature-feedback capability was demonstrated in photothermal therapy with precise control of temperature. This temperature-feedback upconversion nanotechnology was also expanded to programmable therapy combining chemo and photothermal therapeutic models.[46]

3.4. Immunotherapy

In recent years, immunotherapy has become recognized as a promising paradigm for antitumor growth and especially for metastasis. Immunotherapy stimulates the functions of immune systems and improves the body's natural ability to fight cancer. However, conventional immunomodulation presents off-tumor toxicity, unsatisfactory immune response, and adverse autoimmune effects. To achieve a stronger immune response, phototherapeutic pretreatment is generally carried out before immunoregulation because it supplies tumor-associated antigens and a suitable immunological microenvironment in lesions through initial tumor cell deaths. Recently, a large-pore, mesoporous silica nanoplatform, comprising an upconversion nanotransducer, photosensitizing molecule, adjuvant, and vaccine antigen, was employed as a multifunctional immune activator to boost synergistic immunopotentiation and enhance cancer immunotherapy.[47] In 2019, our group synthesized polydopamine-encapsulated upconversion nanoparticles for antitumor immunity and antimetastatic activation through introduction of synergistic photodynamic and photothermal therapeutic modalities, which exploited energy conversion from the as-designed upconversion nanoparticles (Figure 6b).[48] Another study of ours demonstrated that integration of upconversion nanoparticles and aggregation-induced emission molecules showed potent immune activation for antitumor therapy through dual-modal

https://dx.doi.org/10.1021/acs.accounts.0c00513
Acc. Chem. Res. 2020, 53, 2692−2704

ROS generation under NIR irradiation at different power densities (Figure 6c).[2] In this study, the high-dose ROS mode resulted in immunogenic cell death and tumor-associated antigen release. In contrast, the low-dose ROS mode efficiently activated T cell immune responses, simultaneously inhibiting tumor recurrence and metastasis. In 2019, a nanomachine made of DNA-conjugated upconversion nanoparticles was explored to demonstrate selective immunomodulation with spatiotemporal control.[49] In this case, immunostimulatory agents were embedded in a single-strand DNA, which only became active after photoactivation of the photocleavable group in the complementary strand. Therefore, the immunodevice provides a noninvasive strategy to remotely control adjuvant activity with high spatiotemporal precision to reduce systemic toxicity. However, these above-mentioned strategies rely on one or several selected tumor-associated antigens, inevitably running the risk of failure to generate an immune response due to tumor heterogeneity.

3.5. Drug Delivery

Despite significant progress in cancer therapeutics, chemotherapy remains preferred in clinical anticancer practice. However, chemotherapy usually involves poor drug solubility, elusive dosage administration, drug tolerance issues, and contraindications. A reliable and efficient drug delivery system is expected to address these concerns and becomes indispensable to precision nanomedicine in chemotherapy. Key parameters that assess the performance of such systems include, but are not limited to, biocompatibility, loading capacity for therapeutic molecules, premature leakage inhibition of drugs prior to stimulus-activation, response sensitivity to stimuli, and dynamic control of drug release. Stimulus-responsive nanotechnology has proven efficacious, in that drug release can be triggered by endogenous characteristics of the tumor microenvironment or exogenous photonic/vibrational energy. In a recent study, upconversion luminescence-induced azo-photoisomerization was used to remotely control release kinetics of drugs intercalated into DNA helices.[50] In this case, perinuclear aggregation of drugs was achieved through additional functionalization with a nuclear-targeting peptide and hyaluronic acid on the surface of the nanoplatform. In another example, drug release was precisely administered through temperature-feedback photothermal modulation, utilizing phonon-responsive upconversion emission.[46]

The stimulus-responsive nanoplatform can also deliver metal ions (e.g., Mn^{2+}, Fe^{2+}, and Zn^{2+}) or biomolecules (e.g., prodrugs and nucleic acids) for specific or synergistic oncotherapeutics. For example, tumor-targeted and intramitochondrial release of Fe^{2+} ions promoted the generation of hydroxyl radicals through upconverting photocatalyzed Fenton-like reactions, resulting in apoptosis and ferroptosis of tumor cells due to damage of mitochondrial DNA.[51] Recently, upconversion nanoparticles conjugated with a ferric−gallic acid complex were demonstrated as pH-sensitive probes for synergistic antitumor therapy, in which complex and unsaturated ferric ions contributed to photothermal conversion and a Fenton-like reaction assisted photodynamic therapy, respectively.[52] In addition, an upconversion nanoparticle-based delivery system also can be applied in gene delivery. Near-infrared light modulation of upconversion nanoprobes was also established as a remote-controllable gene editing platform for on-demand release of clustered, regularly interspaced short palindromic repeats and CRISPR-associated protein 9 (CRISPR-Cas9) in deep tissue (Figure 6d).[53] However, such photoluminescence-derived CRISPR strategies raise concerns over the physicochemical stability of the delivering system, penetration depths of the stimulatory light, and the response efficacy of gene editing *in vivo*.

4. NEUROMODULATION

Apart from oncotherapy, lanthanide-activated nanoprobes have been employed in other treatments such as wound recovery, bacterial infection, neurodegenerative disorders, and aging-related diseases. In a recent study, hyaluronate−rose bengal-conjugated upconversion nanocomplexes promoted non-invasive, photochemically stimulated tissue bonding in deep tissue, compared with conventional suturing and stapling strategies.[54] In addition, *in vivo* infection by pathogenic bacteria can be effectively regulated by remote and reversible interference of bacterial−cell interactions through near-infrared light modulation.[55] Photomodulation of C_{60}-capped upconversion nanocomplexes enabled amyloid beta photo-oxygenation and protection against excessive oxidative stress for Alzheimer's disease treatment.[39] Recently, accelerated clearance of senescent cells, as a theranostic approach to aging-related diseases, was demonstrated through administration of a DNA-mediated nanoarchitecture comprising Au-upconversion nanoparticles, in which beta-2-microglobulin antibody recognition induced exposure of granzyme B for senescent cell apoptosis.[56]

Optogenetics is a specific, high-resolution targeting technique to spatiotemporally regulate neural activities by stimulating photosensitive opsin proteins of targeted neurons genetically encoded in cellular membranes. Opsins modulate cation or anion flow via light-gated ion channels that change conformation upon photostimulation, resulting in neural excitation or inhibition and activation of cellular signaling pathways. In contrast to invasive delivery of visible light in conventional optogenetic approaches, upconversion nanoplatforms enable near-infrared-mediated optogenetics with wireless control.[57] Upconversion-mediated optogenetics offers advantages of precise, remote control of targeted neurons or areas, minimal invasion, and reduced tissue damage as well as reduced inflammatory response by the body.

Remote manipulation of neural activity was first demonstrated in *in vitro* cell culture systems and then in transparent *in vivo* models such as *Caenorhabditis elegans* and zebrafish.[57] An early demonstration in mammals for transcranial deep brain neuromodulation was devoted to behavioral regulation of freely moving rodents after implantation of upconversion nanoparticle-encapsulated micro-optrodes.[58] In 2018, our group developed a minimally invasive strategy to multiplex deep brain neuromodulation in rodents through direct transcranial injection of upconversion nanoprobes into the hippocampi of transgenic mice (Figure 7a,b).[3] In this work, dopamine-regulated fear memory recollection was activated by ChR2-expressing neurons upon upconverted visible light, and fear-induced freezing behavior was also observed in the freely moving mice (Figure 7c,d). Recently, upconversion nanoparticle-mediated optogenetics was also demonstrated to overcome physiological visual limits in rodent models.[59] After ocular injection of photoreceptor-binding upconversion nanoparticles, the mice could recognize NIR light and patterns without affecting the native daylight vision. This finding may provide an alternative treatment for ophthalmic diseases.

https://dx.doi.org/10.1021/acs.accounts.0c00513
Acc. Chem. Res. 2020, 53, 2692−2704

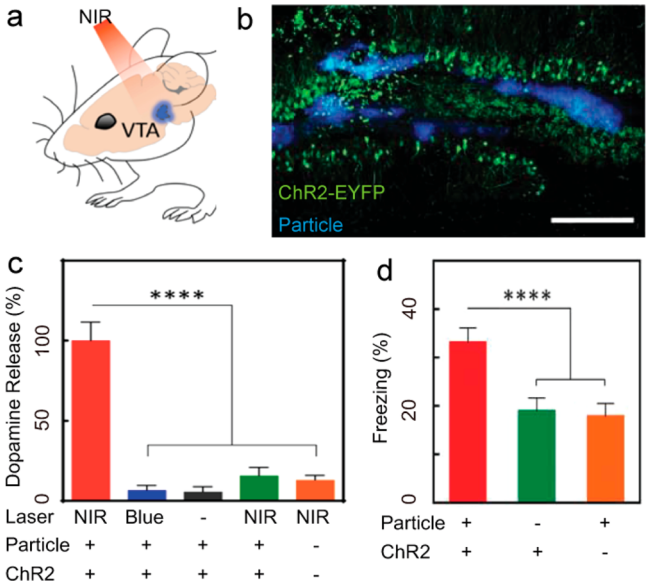

Figure 7. Lanthanide-activated nanoparticles in optogenetics. (a) Schematic illustration showing transcranial stimulation of dopamine neurons in the ventral tegmental area (VTA). (b) Confocal image showing the overlap between upconversion nanoparticles and ChR2 expression. Scale bar: 200 μm. (c) Dopamine release profile and (d) freezing level of different experimental groups. Adapted with permission from ref 3. Copyright 2018 American Association for the Advancement of Science.

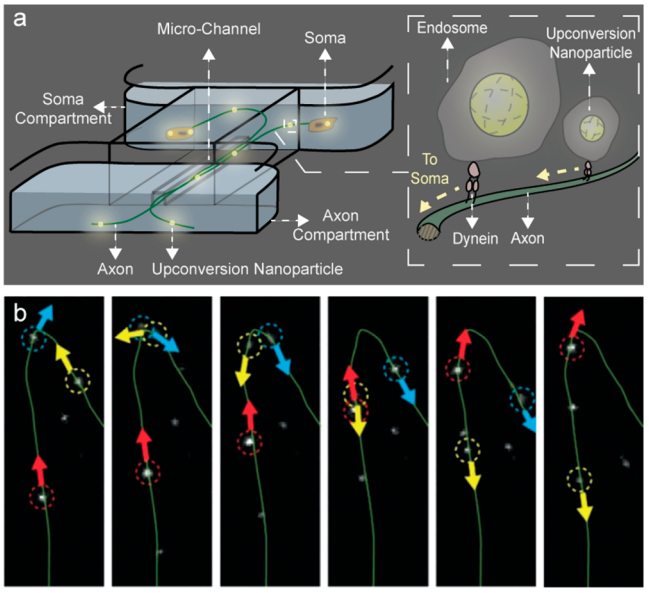

Figure 8. Lanthanide-activated nanoparticles in intraneural tracing. (a) Scheme of two-compartment neural culture system and an illustration showing upconversion nanoparticles moving along a microtubule in axons. (b) Optical tracing of upconversion luminescence in an axon, where the red and green arrows indicate retrograde transport while the yellow one presents anterograde transport. Adapted with permission from ref 4. Copyright 2019 WILEY-VCH Verlag GmbH & Co. KGaA.

We also successfully expanded this strategy to inhibit neural circuitry and provoke hippocampal theta-oscillations. Non-significant cytotoxicity from nanoparticles and photostimulation demonstrated the practical potential of *in vivo* upconversion-mediated optogenetics, especially in transcranial neurostimulation and neurological treatment. Apart from neuromodulation, upconversion nanoparticles can also be used in labeling intraneural cargos to visualize their trafficking details under microscopy. In 2019, we demonstrated real-time monitoring of intraneuronal motor protein transport by tracking the movement of upconversion nanoparticles.[4] This technique benefited from the two-compartment neural culture system in which we can efficiently separate the soma and axons into two parts (Figure 8a). Bright upconversion luminescence led to quantitative tracking of retro- and anterograde transport with single-particle resolution at a monitoring frequency of 7 Hz (Figure 8b). Statistical analysis of transportation features provided the clue to early-stage diagnosis of neurodegenerative disorders, such as Rett syndrome. Upconversion microscopy simultaneously provides an advanced assessment technique for neurotoxicity, which may contribute to drug discovery and screening.

5. CONCLUSIONS AND OUTLOOK

In the past five years, research on lanthanide-activated nanoparticles has gained considerable momentum with systematic *in vitro* and *in vivo* investigations in multifunctional bioimaging, phototherapy, and optogenetics, illuminating their promise in precision nanomedicine in the near future. Key challenges to expanding the use of new-generation nanoprobes in diverse bioapplications include the following: (i) Brightness or quantum efficiency of upconversion emissions and maintaining their optical performance after hydrophilic surface treatment need to be improved. Although several strategies have proven effective for luminescence enhancement, further improvement is needed.[60] (ii) *In vivo* biocompatibility of nanoprobes to combat probe-induced cytotoxicity must be enhanced. Efforts should be focused on surface science and biointerfacing through advanced nanotechnology and biological methodology. (iii) It is important to establish "gold standards" to assess biosafety and diagnostic and therapeutic performance of as-exploited nanoplatforms. Thus far, bioapplications of lanthanide-based nanoprobes have only been demonstrated at cellular and small-animal levels. There are limited studies on large animals such as macaques and at preclinical levels. (iv) Multidisciplinary investigations integrating new knowledge and technologies may unlock infinite possibilities for lanthanide-activated nanoprobes in new eras of nanomedicine.

AUTHOR INFORMATION

Corresponding Author

Xiaogang Liu − *Department of Chemistry and The N.1 Institute for Health, National University of Singapore, Singapore 117543 Singapore; Center for Functional Materials, National University of Singapore Suzhou Research Institute, Suzhou 215123, China;* orcid.org/0000-0003-2517-5790; Email: chmlx@nus.edu.sg

Authors

Zhigao Yi − *Department of Chemistry and The N.1 Institute for Health, National University of Singapore, Singapore 117543 Singapore;* orcid.org/0000-0003-0853-2055

Zichao Luo − *Department of Chemistry and The N.1 Institute for Health, National University of Singapore, Singapore 117543 Singapore;* orcid.org/0000-0001-9236-9160

https://dx.doi.org/10.1021/acs.accounts.0c00513
Acc. Chem. Res. 2020, 53, 2692−2704

Xian Qin − *Department of Chemistry, National University of Singapore, Singapore 117543 Singapore;* orcid.org/0000-0001-8569-7721

Qiushui Chen − *Department of Chemistry, National University of Singapore, Singapore 117543 Singapore;* orcid.org/0000-0002-3039-2098

Complete contact information is available at: https://pubs.acs.org/10.1021/acs.accounts.0c00513

Funding

This work was supported by the Singapore Ministry of Education (MOE2017-T2-2-110), Agency for Science, Technology and Research (A*STAR) (A1883c0011 and A1983c0038), National Research Foundation, Prime Minister's Office, Singapore under the NRF Investigatorship Programme (Award NRF-NRFI05−2019−0003), and National Natural Science Foundation of China (21771135).

Notes

The authors declare no competing financial interest.

Biographies

Zhigao Yi obtained his B.S. degree in Packaging Materials and Engineering from Hunan University of Science and Technology, China. He received his M.S. degree in Materials Science and Engineering from Xiangtan University, China, and completed his Ph.D. study in the research group of Prof. Xiaogang Liu at National University of Singapore in 2019. He is currently a research assistant at National University of Singapore. His current research interests focus on the design of multifunctional nanomaterials for bioimaging, phototherapy, and neuromodulation.

Zichao Luo earned his B.S. degree in Biotechnology from Xinyang Normal University. He received his M.Sc. degree in Cellular Biology from Sichuan University in 2011 and then joined Chinese Academy of Science as a research assistant, developing novel nanomaterials and supramolecular hydrogels as anticancer vaccines. He is currently pursuing a Ph.D. in Chemistry under the supervision of Prof. Xiaogang Liu at National University of Singapore. His current research interests include the synthesis of polymeric nanomaterials and upconversion nanoparticles for bioimaging, photodynamic therapy, and immunotherapy.

Xian Qin earned her B.S. degree (2007) in Mechanical Engineering from Sichuan University. She received her Ph.D. under the supervision of Prof. Qingyuan Meng in 2013 from Harbin Institute of Technology, China. She subsequently carried out postdoctoral training in Chemistry Department at National University of Singapore and also Institute of Materials Research and Engineering (IMRE) at A*STAR, Singapore. Her current research is focused on molecular optoelectronics, low-dimensional systems design and Brownian motion, as well as quantum and classical methodologies for understanding optical properties of luminescent nanomaterials.

Qiushui Chen received his B.Sc. degree in Chemistry from Fuzhou University in 2009 and Ph.D. in Chemistry from Tsinghua University in 2014. He then joined the group of Prof. Xiaogang Liu as a research fellow at National University of Singapore in 2015. His research interests are inorganic luminescence nanocrystals and their use for optical imaging.

Xiaogang Liu received his B.E. degree in Chemical Engineering from Beijing Technology and Business University, China. He received his M.S. degree in Chemistry from East Carolina University and completed his Ph.D. at Northwestern University. He then carried out postdoctoral work at MIT for two years before joining the National University of Singapore in 2006. Currently, he sits as an Associate Editor for Nanoscale and serves on the editorial boards of Research, Chemistry—An Asian Journal, Advanced Optical Materials, Journal of Luminescence, and Journal of Physical Chemistry Letters. His research encompasses areas including nanostructured catalysis, optical nanomaterials, optogenetic neuromodulation, and X-ray imaging.

REFERENCES

(1) Yi, Z.; Luo, Z.; Barth, N. D.; Meng, X.; Liu, H.; Bu, W.; All, A.; Vendrell, M.; Liu, X. *In Vivo* Tumor Visualization through MRI Off-On Switching of $NaGdF_4$-$CaCO_3$ Nanoconjugates. *Adv. Mater.* **2019**, *31*, 1901851.

(2) Mao, D.; Hu, F.; Yi, Z.; Kenry; Xu, S.; Yan, S.; Luo, Z.; Wu, W.; Wang, Z.; Kong, D.; Liu, X.; Liu, B. AIEgen-Coupled Upconversion Nanoparticles Eradicate Solid Tumors through Dual-Mode ROS Activation. *Sci. Adv.* **2020**, *6* (6), eabb2712.

(3) Chen, S.; Weitemier, A. Z.; Zeng, X.; He, L.; Wang, X.; Tao, Y.; Huang, A. J.; Hashimotodani, Y.; Kano, M.; Iwasaki, H.; Parajuli, L. K.; Okabe, S.; Teh, D. B. L.; All, A. H.; Tsutsui-Kimura, I.; Tanaka, K. F.; Liu, X.; McHugh, T. J. Near-Infrared Deep Brain Stimulation via Upconversion Nanoparticle-Mediated Optogenetics. *Science* **2018**, *359*, 679−684.

(4) Zeng, X.; Chen, S.; Weitemier, A.; Han, S.; Blasiak, A.; Prasad, A.; Zheng, K.; Yi, Z.; Luo, B.; Yang, I. H.; Thakor, N.; Chai, C.; Lim, K. L.; McHugh, T. J.; All, A. H.; Liu, X. Visualization of Intra-Neuronal Motor Protein Transport through Upconversion Microscopy. *Angew. Chem., Int. Ed.* **2019**, *58*, 9262−9268.

(5) Auzel, F. Upconversion and Anti-Stokes Processes with f and d Ions in Solids. *Chem. Rev.* **2004**, *104*, 139−174.

(6) Qin, X.; Xu, J.; Wu, Y.; Liu, X. Energy-Transfer Editing in Lanthanide-Activated Upconversion Nanocrystals: A Toolbox for Emerging Applications. *ACS Cent. Sci.* **2019**, *5*, 29−42.

(7) Fan, Y.; Wang, P.; Lu, Y.; Wang, R.; Zhou, L.; Zheng, X.; Li, X.; Piper, J. A.; Zhang, F. Lifetime-Engineered NIR-II Nanoparticles Unlock Multiplexed *In Vivo* Imaging. *Nat. Nanotechnol.* **2018**, *13*, 941−946.

(8) Gu, Y.; Guo, Z.; Yuan, W.; Kong, M.; Liu, Y.; Liu, Y.; Gao, Y.; Feng, W.; Wang, F.; Zhou, J.; Jin, D.; Li, F. High-Sensitivity Imaging of Time-Domain Near-Infrared Light Transducer. *Nat. Photonics* **2019**, *13*, 525−531.

(9) Uh, H.; Petoud, S. Novel Antennae for the Sensitization of Near Infrared Luminescent Lanthanide Cations. *C. R. Chim.* **2010**, *13*, 668−680.

(10) Xie, X.; Gao, N.; Deng, R.; Sun, Q.; Xu, Q. H.; Liu, X. Mechanistic Investigation of Photon Upconversion in Nd^{3+}-Sensitized Core-Shell Nanoparticles. *J. Am. Chem. Soc.* **2013**, *135*, 12608−12611.

(11) Wang, Y.; Liu, G.; Sun, L.; Xiao, J.; Zhou, J.; Yan, C. Nd(3+)-Sensitized Upconversion Nanophosphors: Efficient *In Vivo* Bioimaging Probes with Minimized Heating Effect. *ACS Nano* **2013**, *7*, 7200−7206.

(12) Chen, Q.; Xie, X.; Huang, B.; Liang, L.; Han, S.; Yi, Z.; Wang, Y.; Li, Y.; Fan, D.; Huang, L.; Liu, X. Confining Excitation Energy in Er^{3+}-Sensitized Upconversion Nanocrystals through Tm^{3+}-Mediated Transient Energy Trapping. *Angew. Chem., Int. Ed.* **2017**, *56*, 7605−7609.

(13) Zheng, K.; Han, S.; Zeng, X.; Wu, Y.; Song, S.; Zhang, H.; Liu, X. Rewritable Optical Memory Through High-Registry Orthogonal Upconversion. *Adv. Mater.* **2018**, *30*, 1801726.

(14) Liang, L.; Teh, D. B.; Dinh, N. D.; Chen, W.; Chen, Q.; Wu, Y.; Chowdhury, S.; Yamanaka, A.; Sum, T. C.; Chen, C. H.; Thakor, N.; All, A. H.; Liu, X. Upconversion Amplification through Dielectric Superlensing Modulation. *Nat. Commun.* **2019**, *10*, 1391.

(15) Wu, Y.; Xu, J.; Poh, E. T.; Liang, L.; Liu, H.; Yang, J.; Qiu, C.; Vallée, R. A.; Liu, X. Upconversion Superburst with Sub-2 μs Lifetime. *Nat. Nanotechnol.* **2019**, *14*, 1110−1115.

(16) Deng, R.; Qin, F.; Chen, R.; Huang, W.; Hong, M.; Liu, X. Temporal Full-Colour Tuning through Non-Steady-State Upconversion. *Nat. Nanotechnol.* **2015**, *10*, 237−242.
(17) Zhong, Y.; Ma, Z.; Zhu, S.; Yue, J.; Zhang, M.; Antaris, A. L.; Yuan, J.; Cui, R.; Wan, H.; Zhou, Y.; Huang, N. F.; Luo, J.; Hu, Z.; Dai, H. Boosting the Down-Shifting Luminescence of Rare-Earth Nanocrystals for Biological Imaging beyond 1500 nm. *Nat. Commun.* **2017**, *8*, 737.
(18) Li, Y.; Zeng, S.; Hao, J. Non-Invasive Optical Guided Tumor Metastasis/Vessel Imaging by Using Lanthanide Nanoprobe with Enhanced Down-Shifting Emission beyond 1500 nm. *ACS Nano* **2019**, *13*, 248−259.
(19) Zhong, Y.; Ma, Z.; Wang, F.; Wang, X.; Yang, Y.; Liu, Y.; Zhao, X.; Li, J.; Du, H.; Zhang, M.; Cui, Q.; Zhu, S.; Sun, Q.; Wan, H.; Tian, Y.; Liu, Q.; Wang, W.; Garcia, K. C.; Dai, H. *In Vivo* Molecular Imaging for Immunotherapy Using Ultra-Bright Near-Infrared-IIb Rare-Earth Nanoparticles. *Nat. Biotechnol.* **2019**, *37*, 1322−1331.
(20) Qiu, X.; Zhu, X.; Xu, M.; Yuan, W.; Feng, W.; Li, F. Hybrid Nanoclusters for Near-Infrared to Near-Infrared Upconverted Persistent Luminescence Bioimaging. *ACS Appl. Mater. Interfaces* **2017**, *9*, 32583−32590.
(21) Liu, Y.; Ai, K.; Liu, J.; Yuan, Q.; He, Y.; Lu, L. A High-Performance Ytterbium Based Nanoparticulate Contrast Agent for *In Vivo* X-Ray Computed Tomography Imaging. *Angew. Chem., Int. Ed.* **2012**, *51*, 1437−1442.
(22) Naczynski, D. J.; Sun, C.; Türkcan, S.; Jenkins, C.; Koh, A. L.; Ikeda, D.; Pratx, G.; Xing, L. X-Ray-Induced Shortwave Infrared Biomedical Imaging Using Rare-Earth Nanoprobes. *Nano Lett.* **2015**, *15*, 96−102.
(23) Mi, Z.; Zhang, Y.; Vanga, S. K.; Chen, C.; Tan, H.; Watt, F.; Liu, X.; Bettiol, A. A. Subwavelength Imaging through Ion-Beam-Induced Upconversion. *Nat. Commun.* **2015**, *6*, 8832.
(24) Xing, H.; Zhang, S.; Bu, W.; Zheng, X.; Wang, L.; Xiao, Q.; Ni, D.; Zhang, J.; Zhou, L.; Peng, W.; Zhao, K.; Hua, Y.; Shi, J. Ultrasmall $NaGdF_4$ Nanodots for Efficient MR Angiography and Atherosclerotic Plaque Imaging. *Adv. Mater.* **2014**, *26*, 3867−3872.
(25) Zhang, X.; Blasiak, B.; Marenco, A. J.; Trudel, S.; Tomanek, B.; van Veggel, F. C. Design and Regulation of $NaHoF_4$ and $NaDyF_4$ Nanoparticles for High-Field Magnetic Resonance Imaging. *Chem. Mater.* **2016**, *28*, 3060−3072.
(26) Yi, Z.; Li, X.; Lu, W.; Liu, H.; Zeng, S.; Hao, J. Hybrid Lanthanide Nanoparticles as a New Class of Binary Contrast Agents for *In Vivo* T_1/T_2 Dual-Weighted MRI and Synergistic Tumor Diagnosis. *J. Mater. Chem. B* **2016**, *4*, 2715−2722.
(27) Ovais, M.; Mukherjee, S.; Pramanik, A.; Das, D.; Mukherjee, A.; Raza, A.; Chen, C. Designing Stimuli-Responsive Upconversion Nanoparticles that Exploit the Tumor Microenvironment. *Adv. Mater.* **2020**, *32*, 2000055.
(28) Wang, Y.; Song, S.; Liu, J.; Liu, D.; Zhang, H. ZnO-Functionalized Upconverting Nanotheranostic Agent: Multi-Modality Imaging-Guided Chemotherapy with On-Demand Drug Release Triggered by pH. *Angew. Chem., Int. Ed.* **2014**, *54*, 536−540.
(29) Zhao, J.; Li, Y.; Yu, M.; Gu, Z.; Li, L.; Zhao, Y. Time-Resolved Activation of pH Sensing and Imaging *In Vivo* by Remotely Controllable DNA Nanomachine. *Nano Lett.* **2020**, *20*, 874−880.
(30) Wang, P.; Li, X.; Yao, C.; Wang, W.; Zhao, M.; El-Toni, A. M.; Zhang, F. Orthogonal Near-Infrared Upconversion Co-Regulated Site-Specific O_2 Delivery and Photodynamic Therapy for Hypoxia Tumor by Using Red Blood Cell Microcarriers. *Biomaterials* **2017**, *125*, 90−100.
(31) Luo, C.; Huang, C.; Su, C.; Yeh, C. Bacteria-Mediated Hypoxia-Specific Delivery of Nanoparticles for Tumors Imaging and Therapy. *Nano Lett.* **2016**, *16*, 3493−3499.
(32) Liu, Y.; Liu, Y.; Bu, W.; Cheng, C.; Zuo, C.; Xiao, Q.; Sun, Y.; Ni, D.; Zhang, C.; Liu, J.; Shi, J. Hypoxia Induced by Upconversion-Based Photodynamic Therapy: Towards Highly Effective Synergistic Bioreductive Therapy in Tumors. *Angew. Chem., Int. Ed.* **2015**, *54*, 8105−8109.
(33) Wan, W.; Tian, B.; Lin, Y.; Korupalli, C.; Lu, M.; Cui, Q.; Wan, D.; Chang, Y.; Sung, H. W. Photosynthesis-Inspired H_2 Generation Using a Chlorophyll-Loaded Liposomal Nanoplatform to Detect and Scavenge Excess ROS. *Nat. Commun.* **2020**, *11*, 534.
(34) Peng, J.; Samanta, A.; Zeng, X.; Han, S.; Wang, L.; Su, D.; Loong, D. T. B.; Kang, N.; Park, S. J.; All, A. H.; Jiang, W.; Yuan, L.; Liu, X.; Chang, Y. T. Real-Time *In Vivo* Hepatotoxicity Monitoring through Chromophore-Conjugated Photon-Upconverting Nanoprobes. *Angew. Chem., Int. Ed.* **2017**, *56*, 4165−4169.
(35) Shi, Z.; Zhang, K.; Zada, S.; Zhang, C.; Meng, X.; Yang, Z.; Dong, H. Upconversion Nanoparticle-Induced Multimode Photodynamic Therapy Based on a Metal−Organic Framework/Titanium Dioxide Nanocomposite. *ACS Appl. Mater. Interfaces* **2020**, *12*, 12600−12608.
(36) Fan, W.; Bu, W.; Shen, B.; He, Q.; Cui, Z.; Liu, Y.; Zheng, X.; Zhao, K.; Shi, J. Intelligent MnO_2 Nanosheets Anchored with Upconversion Nanoprobes for Concurrent pH-/H_2O_2-Responsive UCL Imaging and Oxygen-Elevated Synergetic Therapy. *Adv. Mater.* **2015**, *27*, 4155−4161.
(37) Yao, C.; Wang, W.; Wang, P.; Zhao, M.; Li, X.; Zhang, F. Near-Infrared Upconversion Mesoporous Cerium Oxide Hollow Biophotocatalyst for Concurrent pH-/H_2O_2-Responsive O_2-Evolving Synergetic Cancer Therapy. *Adv. Mater.* **2018**, *30*, 1704833.
(38) Shen, T.; Hu, X.; Liu, Y.; Zhang, Y.; Chen, K.; Xie, S.; Ke, G.; Song, G.; Zhang, X. Specific Core-Satellite Nanocarriers for Enhanced Intracellular ROS Generation and Synergistic Photodynamic Therapy. *ACS Appl. Mater. Interfaces* **2020**, *12* (5), 5403−5412.
(39) Du, Z.; Gao, N.; Wang, X.; Ren, J.; Qu, X. Near-Infrared Switchable Fullerene-Based Synergy Therapy for Alzheimer's Disease. *Small* **2018**, *14*, 1801852.
(40) Lai, J.; Shah, B. P.; Zhang, Y.; Yang, L.; Lee, K. B. Real-Time Monitoring of ATP-Responsive Drug Release Using Mesoporous-Silica-Coated Multicolor Upconversion Nanoparticles. *ACS Nano* **2015**, *9*, 5234−5245.
(41) Zhao, J.; Gao, J.; Xue, W.; Di, Z.; Xing, H.; Lu, Y.; Li, L. Upconversion Luminescence-Activated DNA Nanodevice for ATP Sensing in Living Cells. *J. Am. Chem. Soc.* **2018**, *140*, 578−581.
(42) Li, F.; Du, Y.; Liu, J.; Sun, H.; Wang, J.; Li, R.; Kim, D.; Hyeon, T.; Ling, D. Responsive Assembly of Upconversion Nanoparticles for pH-Activated and Near-Infrared-Triggered Photodynamic Therapy of Deep Tumors. *Adv. Mater.* **2018**, *30*, 1802808.
(43) Ai, X.; Ho, C. J. H.; Aw, J.; Attia, A. B. E.; Mu, J.; Wang, Y.; Wang, X.; Wang, Y.; Liu, X.; Chen, H.; Gao, M.; Chen, X.; Yeow, E. K. L.; Liu, G.; Olivo, M.; Xing, B. *In Vivo* Covalent Cross-Linking of Photon-Converted Rare-Earth Nanostructures for Tumour Localization and Theranostics. *Nat. Commun.* **2016**, *7*, 10432.
(44) He, L.; Ni, Q.; Mu, J.; Fan, W.; Liu, L.; Wang, Z.; Li, L.; Tang, W.; Liu, Y.; Cheng, Y.; Tang, L. Solvent-Assisted Self-Assembly of a Metal-Organic Framework Based Biocatalyst for Cascade Reaction Driven Photodynamic Therapy. *J. Am. Chem. Soc.* **2020**, *142*, 6822−6832.
(45) Han, S.; Samanta, A.; Xie, X.; Huang, L.; Peng, J.; Park, S. J.; Teh, D. B. L.; Choi, Y.; Chang, Y. T.; All, A. H.; Yang, Y.; Xing, B.; Liu, X. Gold and Hairpin DNA Functionalization of Upconversion Nanocrystals for Imaging and *In Vivo* Drug Delivery. *Adv. Mater.* **2017**, *29*, 1700244.
(46) Zhu, X.; Li, J.; Qiu, X.; Liu, Y.; Feng, W.; Li, F. Upconversion Nanocomposite for Programming Combination Cancer Therapy by Precise Control of Microscopic Temperature. *Nat. Commun.* **2018**, *9*, 2176.
(47) Ding, B.; Shao, S.; Yu, C.; Teng, B.; Wang, M.; Cheng, Z.; Wong, K. L.; Ma, P.; Lin, J. Large-Pore Mesoporous-Silica-Coated Upconversion Nanoparticles as Multifunctional Immunoadjuvants with Ultrahigh Photosensitizer and Antigen Loading Efficiency for Improved Cancer Photodynamic Immunotherapy. *Adv. Mater.* **2018**, *30*, 1802479.
(48) Yan, S.; Zeng, X.; Tang, Y.; Liu, B.; Wang, Y.; Liu, X. Activating Antitumor Immunity and Antimetastatic Effect through Polydop-

https://dx.doi.org/10.1021/acs.accounts.0c00513
Acc. Chem. Res. 2020, 53, 2692−2704

amine-Encapsulated Core-Shell Upconversion Nanoparticles. *Adv. Mater.* **2019**, *31*, 1905825.
(49) Chu, H.; Zhao, J.; Mi, Y.; Di, Z.; Li, L. NIR-Light-Mediated Spatially Selective Triggering of Anti-Tumor Immunity via Upconversion Nanoparticle-Based Immunodevices. *Nat. Commun.* **2019**, *10*, 2839.
(50) Zhang, Y.; Zhang, Y.; Song, G.; He, Y.; Zhang, X.; Liu, Y.; Ju, H. A DNA-Azobenzene Nanopump Fueled by Upconversion Luminescence for Controllable Intracellular Drug Release. *Angew. Chem., Int. Ed.* **2019**, *58*, 18207−18211.
(51) Hu, P.; Wu, T.; Fan, W.; Chen, L.; Liu, Y.; Ni, D.; Bu, W.; Shi, J. Near Infrared-Assisted Fenton Reaction for Tumor-Specific and Mitochondrial DNA-Targeted Photochemotherapy. *Biomaterials* **2017**, *141*, 86−95.
(52) Zhang, P.; Hou, Y.; Zeng, J.; Li, Y.; Wang, Z.; Zhu, R.; Ma, T.; Gao, M. Coordinatively Unsaturated Fe^{3+} Based Activatable Probes for Enhanced MRI and Therapy of Tumors. *Angew. Chem., Int. Ed.* **2019**, *58*, 11088−11096.
(53) Pan, Y.; Yang, J.; Luan, X.; Liu, X.; Li, X.; Yang, J.; Huang, T.; Sun, L.; Wang, Y.; Lin, Y.; Song, Y. Near-Infrared Upconversion-Activated CRISPR-Cas9 System: A Remote-Controlled Gene Editing Platform. *Sci. Adv.* **2019**, *5*, eaav7199.
(54) Han, S.; Hwang, B. W.; Jeon, E. Y.; Jung, D.; Lee, G. H.; Keum, D. H.; Kim, K. S.; Yun, S. H.; Cha, H. J.; Hahn, S. K. Upconversion Nanoparticles/Hyaluronate-Rose Bengal Conjugate Complex for Noninvasive Photochemical Tissue Bonding. *ACS Nano* **2017**, *11*, 9979−9988.
(55) Li, W.; Dong, K.; Wang, H.; Zhang, P.; Sang, Y.; Ren, J.; Qu, X. Remote and Reversible Control of *In Vivo* Bacteria Clustering by NIR-Driven Multivalent Upconverting Nanosystems. *Biomaterials* **2019**, *217*, 119310.
(56) Qu, A.; Wu, X.; Li, S.; Sun, M.; Xu, L.; Kuang, H.; Xu, C. An NIR-Responsive DNA-Mediated Nanotetrahedron Enhances the Clearance of Senescent Cells. *Adv. Mater.* **2020**, *32*, 2000184.
(57) All, A. H.; Zeng, X.; Teh, D. B. L.; Yi, Z.; Prasad, A.; Ishizuka, T.; Thakor, N.; Hiromu, Y.; Liu, X. Expanding the Toolbox of Upconversion Nanoparticles for *In Vivo* Optogenetics and Neuromodulation. *Adv. Mater.* **2019**, *31*, 1803474.
(58) Wang, Y.; Lin, X.; Chen, X.; Chen, X.; Xu, Z.; Zhang, W.; Liao, Q.; Duan, X.; Wang, X.; Liu, M.; Wang, F.; He, J.; Shi, P. Tetherless Near-Infrared Control of Brain Activity in Behaving Animals Using Fully Implantable Upconversion Microdevices. *Biomaterials* **2017**, *142*, 136−148.
(59) Ma, Y.; Bao, J.; Zhang, Y.; Li, Z.; Zhou, X.; Wan, C.; Huang, L.; Zhao, Y.; Han, G.; Xue, T. Mammalian near-infrared image vision through injectable and self-powered retinal nanoantennae. *Cell* **2019**, *177*, 243−255.
(60) Liang, L.; Qin, X.; Zheng, K.; Liu, X. Energy Flux Manipulation in Upconversion Nanosystems. *Acc. Chem. Res.* **2019**, *52*, 228−236.

https://dx.doi.org/10.1021/acs.accounts.0c00513
Acc. Chem. Res. 2020, 53, 2692−2704